

Published in final edited form as:
Plant J. 2005 April ; 42(1): 84–94.

microRNA-directed cleavage of *ATHB15* mRNA regulates vascular development in *Arabidopsis* inflorescence stems

Joonki Kim^{1,†}, Jae-Hoon Jung^{1,†}, Jose L. Reyes², Youn-Sung Kim¹, Sun-Young Kim¹, Kyung-Sook Chung¹, Jin A. Kim¹, Minsun Lee¹, Yoontae Lee³, V. Narry Kim³, Nam-Hai Chua², and Chung-Mo Park^{1,*}

¹Graduate School of Chemistry and Molecular Engineering, Seoul National University, Seoul 151-742, South Korea,

²Laboratory of Plant Molecular Biology, Rockefeller University, New York, New York 10021-3699, USA, and

³School of Biological Sciences, Seoul National University, Seoul, 151-742, South Korea

Summary

Class III homeodomain-leucine zipper proteins regulate critical aspects of plant development, including lateral organ polarity, apical and lateral meristem formation, and vascular development. *ATHB15*, a member of this transcription factor family, is exclusively expressed in vascular tissues. Recently, a microRNA (miRNA) binding sequence has been identified in *ATHB15* mRNA, suggesting that a molecular mechanism governed by miRNA binding may direct vascular development through *ATHB15*. Here, we show that miR166-mediated *ATHB15* mRNA cleavage is a principal mechanism for the regulation of vascular development. In a gain-of-function *MIR166a* mutant, the decreased transcript level of *ATHB15* was accompanied by an altered vascular system with expanded xylem tissue and interfascicular region, indicative of accelerated vascular cell differentiation from cambial/procambial cells. A similar phenotype was observed in *Arabidopsis* plants with reduced *ATHB15* expression but reversed in transgenic plants overexpressing an miR166-resistant *ATHB15*. *ATHB15* mRNA cleavage occurred in standard wheat germ extracts and in *Arabidopsis* and was mediated by miR166 in *Nicotiana benthamiana* cells. miR166-assisted *ATHB15* repression is likely to be a conserved mechanism that regulates vascular development in all vascular plants.

Keywords

Arabidopsis; *ATHB15*; HD-ZIP; microRNA; mRNA cleavage; vascular development

Introduction

Vascular system is an elaborate network of conducting tissues that interconnects all plant organs and transports water, minerals, organic compounds, and signaling molecules throughout the plant body. It consists of two conducting tissues, xylem and phloem, and procambial/cambial cells.

Vascular development is initiated by the formation of provascular cells that subsequently develop into procambium, from which both conducting tissues are eventually differentiated (Steeves and Sussex, 1989). In older plant parts, vascular tissues can develop through the

*For correspondence (fax +82 2 889 1568; e-mail cmpark@snu.ac.kr).

†The contribution of these authors should be considered equal.

activity of a secondary meristem, called vascular cambium (Esau, 1965). Plant growth hormones, such as auxins and brassinosteroids, also play regulatory roles in vascular tissue differentiation (Carland *et al.*, 2002; Jang *et al.*, 2000; Sachs, 2000). It is now generally accepted that a unified molecular mechanism modulates temporal and spatial development of vascular tissues in different plant species, although vascular patterns and organizations are quite diverse (Baima *et al.*, 2001). However, the molecular components and schemes that regulate vascular development are poorly understood.

Recent application of molecular genetic tools, mainly established in Arabidopsis, greatly accelerated the identification of genes involved in vascular development and the elucidation of regulatory mechanisms at the molecular level. A subset of class III homeodomain-leucine zipper (HD-ZIP III) transcription factors has been implicated in vascular development. In Arabidopsis, the HD-ZIP III gene family includes five members; *ATHB15*, *ATHB8*, *PHAVOLUTA (PHV)*, *PHABULOSA (PHB)*, and *REVOLUTA (REV)*. *PHV*, *PHB*, and *REV* are expressed in various plant tissues, including vascular tissues, apical and floral meristems, and the adaxial domain of lateral organs (Emery *et al.*, 2003; McConnell *et al.*, 2001; Otsuga *et al.*, 2001). By contrast, *ATHB15* and *ATHB8* are predominantly expressed in vascular tissue (Baima *et al.*, 1995; Ohashi-Ito and Fukuda, 2003), suggesting that they may have some role in vascular development.

ATHB8 is induced by auxin and promotes procambial/ cambial cell differentiation into xylem tissues (Baima *et al.*, 2001). However, a loss-of-function *ATHB8* mutant does not show any defects in vascular patterning and development, indicating that *ATHB8* is not essential for vascular development. Although *ATHB15* has not yet been examined molecular genetically, the predominant expression of *ATHB15* and *ZEHB13*, an *ATHB15* gene homolog from *Zinnia elegans*, in vascular tissue suggests a role for *ATHB15* in vascular development (Ohashi-Ito and Fukuda, 2003). Interestingly, a microRNA (miRNA) binding sequence has been recently predicted in *ATHB15* mRNA (Bartel and Bartel, 2003; Reinhart *et al.*, 2002; Rhoades *et al.*, 2002). It is therefore envisioned that a mechanism governed by miRNA binding might direct the regulatory role of *ATHB15* during vascular development.

miRNAs are small non-coding RNA molecules that regulate target genes by either mRNA cleavage or translational repression (Bartel, 2004; Kidner and Martienssen, 2003). They exert their regulatory role through complementary base pairing to target mRNAs. A handful of miRNAs and their target genes have been identified and demonstrated to regulate various plant developmental processes in recent years, including flowering time control, floral development, leaf polarity, and leaf morphogenesis (Aukerman and Sakai, 2003; Chen, 2004; Emery *et al.*, 2003; Juarez *et al.*, 2004; Kidner and Martienssen, 2004; Laufs *et al.*, 2004; Mallory *et al.*, 2004a,b; McHale and Koning, 2004; Palatnik *et al.*, 2003; Vaucheret *et al.*, 2004). In some cases, the regulatory mechanisms and biochemical actions of miRNAs have been extensively studied using mutants of miRNAs and their target genes. In other cases, only the putative target genes have been studied without functional characterization of the relevant miRNA mutants.

In this work, we isolated an Arabidopsis mutant in which an *MIR166a* gene is activated by the insertion of the CaMV 35S enhancer and demonstrated that miR166-mediated *ATHB15* mRNA cleavage is a principal mechanism for the regulation of vascular development in inflorescence stems. In the gain-of-function *MIR166a* mutant, the *ATHB15* transcript level was drastically reduced, and the vascular system was severely altered with expanded xylem tissue and interfascicular region, indicating that vascular cell differentiation is greatly promoted. *ATHB15* mRNA is cleaved in standard wheat germ extracts and in Arabidopsis, and its cleavage is mediated by miR166 in *Nicotiana benthamiana* cells. The miR166/165 complementary sequence is highly conserved in mRNAs of *ATHB15* and its gene homologs from various plant

species (Floyd and Bowman, 2004). It is therefore likely that miR166-mediated HD-ZIP III gene repression is conserved in all vascular plants.

Results

Isolation of the *men1* mutation

To explore the molecular genetic components and regulatory mechanisms that govern plant growth and development, we generated an Arabidopsis mutant pool by randomly integrating the CaMV 35S enhancer into the genome of Columbia accession (Col-0) (Weigel *et al.*, 2000). We then searched for morphogenetic mutants with altered leaf and inflorescence stem morphologies. Among the isolated mutants, we chose a morphogenetic mutant with severe growth retardation.

The mutant, designated *men1* for *meristem enlargement 1*, exhibits pleiotropic alterations in the inflorescence stem and leaf morphologies and floral structure in addition to repressed growth (Figure 1). Homozygous *men1* lines stopped growing at the very early seedling stage (<1 cm in height) and eventually died without further development in most lines. Although one or two flowers were occasionally produced in a few lines, they were sterile, possibly due to extremely short carpels (Figure 2c). When homozygous *men1* plants were pollinated with wild-type pollens, no seeds were produced. However, seeds were successfully produced from wild-type plants pollinated with homozygous *men1* pollens (data not shown). Therefore, all experiments were carried out using heterozygous *men1/+* plants.

One prominent feature of *men1/+* is the fasciated inflorescence stem with disrupted radial vascular patterning (Figures 1 and 2a), which may be developmentally related to apical meristem enlargement (Figure 2b). Stem fasciation may be due to disrupted cell partitioning from the central and peripheral zones to the rib zone during shoot apical meristem development (Clark *et al.*, 1996; Laufs *et al.*, 1998). Floral development was also affected by the *men1* mutation. More flowers were produced in *men1/+* than in wild-type plants. In addition, although the numbers of floral organs are unchanged, the carpels are very short and sterile (Figure 2c).

men1 is a gain-of-function MIR166a mutant

Mapping of the T-DNA insertion site by the three-step thermal asymmetric interlaced (TAIL)-PCR (Liu *et al.*, 1995) revealed that the 35S enhancer was inserted into a region between two previously annotated genes *At2g46680* and *At2g46690* (Figure 3a). However, the expression of the two genes was not altered in the mutant, and transgenic plants that express either one of the two genes under the control of the CaMV 35S promoter did not show any phenotypic changes (data not shown), indicating that the phenotypic alterations observed in the mutant are not caused by the misexpression of the two genes.

More careful examination of the intergenic sequence around the T-DNA insertion site resulted in identification of the *MIR166a* gene located about 1.4 kb from the insertion site (Figure 3a). Genomic Southern blot analysis using a genomic DNA fragment as a probe confirmed a single insertion event in the mutant and placed the insertion near the *MIR166a* gene (Figure 3b). Northern blot analysis using an antisense *MIR166a* sequence as a probe revealed that miR166 greatly increased in *men1/+* as well as in *HC-Pro* transgenic plants (Figure 3c), in which the tobacco etch virus helper component proteinase (HC-Pro) is overexpressed (data not shown). This result suggests that miR166 overexpression may be the molecular basis for the *men1* phenotype. We could not recover any viable transgenic plants that overexpress *MIR166a* from four independent transformation attempts. The *MIR166a* gene sequences we tried include the miR166 sequence of 21 bp, a sequence of about 170 bp that contains the flanking genomic DNA sequences of about 75 bp on both sides of the *MIR166a* locus, and genomic DNA

fragments of about 3 and 5 kb that include the *MIR166a* locus in the middle of each fragment. Their expression was driven by the CaMV 35S promoter. A few kanamycin-resistant seeds were obtained, but they died at the very early seedling stage just after germination. This could be because the CaMV 35S promoter-driven miR166 expression is more ubiquitous or more robust than that of the activation tagged lines. However, biochemical actions of miR166 on mRNAs of *ATHB15* and other HD-ZIP III genes and recapitulation of the *men1* phenotype in transgenic plants with reduced *ATHB15* expression unequivocally demonstrate that the *men1* phenotype is caused by miR166 overexpression (see below).

A subset of HD-ZIP III genes is affected by the *men1* mutation

The five HD-ZIP III genes are regulated by miR166/165 in Arabidopsis (Floyd and Bowman, 2004; Mallory *et al.*, 2004b). miR166 directs mRNA cleavage of *PHV* and *PHB* in wheat germ extracts (Tang *et al.*, 2003). *REV* mRNA is cleaved within the miR166/165 binding sequence *in planta* as demonstrated by 5'-RACE experiments (Emery *et al.*, 2003; Zhong and Ye, 2004), although it is currently unclear whether it is cleaved by miR166 or miR165. A similar biochemical mechanism has been proposed in the cleavage of the *ATHB8* and *ATHB15* mRNAs, based on the conservation of the miR166/165 complementary sequences in mRNAs of *ATHB8* and *ATHB15* (Juarez *et al.*, 2004; Reinhart *et al.*, 2002; Rhoades *et al.*, 2002; Zhong and Ye, 2004) (Figure 4a). It has been later demonstrated that their mRNAs are also cleaved by miR165/166 in Arabidopsis through the 5'-RACE method (Mallory *et al.*, 2004b).

To examine the biochemical relationship between miR166 and its target genes, the transcript levels of the target genes were analyzed in *men1*/. Semiquantitative RT-PCR analyses showed that the mRNA levels of *ATHB15* and *PHV* drastically decreased, whereas those of *ATHB8* and *PHB* moderately decreased in *men1*/+ (Figure 4b,c). It is therefore likely that *ATHB15* and *ATHB8* are regulated by miR166 through mRNA cleavage like *PHV* and *PHB*. In particular, *ATHB15* mRNA was barely detectable in *men1*/+, suggesting that at least some features of the *men1* phenotype could be attributed to *ATHB15* functions. The mRNA level of *REV* was identical in *men1*/+ and wild-type plants. *REV* mRNA is cleaved within the miR166/165 target sequence as shown by 5'-RACE experiments, and a semidominant mutation of *REV*, *amphivasal vascular bundle 1 (avb1)*, inhibits the mRNA cleavage (Emery *et al.*, 2003; Zhong and Ye, 2004). It seems that *REV* mRNA is cleaved by miR166/165 in specific plant tissues such as vascular tissues. These observations indicate that the pleiotropic alterations caused by the *men1* mutation are due to multiple effects conferred by *ATHB8*, *PHB*, and *PHV* as well as by *ATHB15*.

ATHB15 is regulated by miR166 through mRNA cleavage

Inflorescence stems are severely fasciated, and vascular differentiation and radial patterning are greatly affected by the *men1* mutation (Figure 2a). Whereas *PHV*, *PHB*, and *REV* are expressed in a broad range of plant tissues (Baima *et al.*, 1995; Emery *et al.*, 2003; McConnell *et al.*, 2001), *ATHB15* and *ATHB8* are expressed more specifically in vascular tissues (Baima *et al.*, 2001; Ohashi-Ito and Fukuda, 2003). Therefore, it is expected that *ATHB15* and *ATHB8* may be more directly related to vascular development than other HD-ZIP III genes. However, it is evident that *ATHB8* is not essential for vascular cell differentiation, although it promotes procambial/cambial cell differentiation into xylem tissues (Baima *et al.*, 2001). These results strongly suggest that miR166-mediated *ATHB15* repression may play a major role in vascular development. We therefore decided to focus on the putative role of *ATHB15* in the regulation of vascular development.

The *ATHB15* transcript level drastically decreased in *men1*/+ (Figure 4b), suggesting that *ATHB15* is regulated by miR166 through mRNA cleavage. We further examined the biochemical relationship between *ATHB15* and miR166 *in vitro* and *in planta*. To more directly

investigate *ATHB15* mRNA cleavage by miR166 in *planta*, an *MIR166a* gene sequence of about 170 bp or the full-size *ATHB15* gene sequences were subcloned under the control of the CaMV 35S promoter in plant expression vector constructs, and the constructs were transformed into *Agrobacterium* cells. The *Agrobacterium* cells were then injected independently or in various combinations into the leaves of *N. benthamiana* for transient expression. Total RNAs were extracted from the leaf tissues at 4 days after injection and analyzed by Northern blot hybridization. *ATHB15* mRNA was cleaved to some extent in the leaf tissues of *N. benthamiana* even in the absence of Arabidopsis miR166, possibly due to intrinsic miR166/165 activity in this plant species. However, it was almost completely cleaved in the presence of Arabidopsis miR166 (Figure 5a, lane 5). By contrast, an *ATHB15* mutant mRNA (*mATHB15*) that has base substitutions within the miR166/165 target sequence but without any amino acid changes (Figure 5c, lane 7) was not cleaved at all by miR166. These results clearly show that *ATHB15* mRNA is cleaved by miR166 through near-perfect base complementarity. *ATHB15* mRNA was also cleaved in standard wheat germ extracts (Figure 5b), indicating that wheat also possesses miR166/165 activity (Tang *et al.*, 2003). It is unclear whether *ATHB15* is also cleaved by miR165.

To confirm the *ATHB15* mRNA cleavage site, the 3'-end cleavage product of *ATHB15* mRNA was isolated from Arabidopsis floral organs, and RNA ligase-mediated 5'-RACE experiments were carried out (Kasschau *et al.*, 2003; Llave *et al.*, 2002). As expected, *ATHB15* mRNA was cleaved within the miR166/165 target sequence that encodes the putative sterol/lipid-binding START domain (Ponting and Aravind, 1999) (Figure 5c). Interestingly, the cleavage site is identical to those confirmed with *PHV* and *REV* mRNAs (Emery *et al.*, 2003; Tang *et al.*, 2003; Zhong and Ye, 2004).

ATHB15 is essential for vascular development

The fasciated inflorescence stems have altered vascular system and radial patterning in *men1/+* (Figure 2). *ATHB15* is primarily expressed in vascular tissues (Baima *et al.*, 1995; Ohashi-Ito and Fukuda, 2003) and regulated by miR166 via mRNA cleavage (Figure 5). Consistent with this, the transcript level of *ATHB15* significantly decreased in *men1/+* (Figure 4b). It is therefore predicted that miR166 directs vascular development by regulating *ATHB15* mRNA.

To investigate the physiological role of *ATHB15* in plant development, especially in vascular development, we generated transgenic Arabidopsis plants that overexpress sense or antisense *ATHB15*. The miR166-resistant *mATHB15* was also included as a control. Overexpression of transgenes and suppression of intrinsic *ATHB15* gene by antisense expression were verified by Northern blot hybridization (Figure 6c). By contrast, it is evident that expression of other HD-ZIP III genes was unaffected in the transgenic plants. The Northern probe was a 483-bp-containing DNA fragment encoding the N-terminal region of *ATHB15*. The observed size difference between the endogenous and the transgenic *ATHB15* transcripts would be due to different sizes of the 5'- and 3'-untranslated sequences.

Sense transgenic plants with *mATHB15* were moderately dwarfed with an upward curling of the leaf blade (Figure 6b). Leaf size was slightly smaller than that of wild-type plants. Transgenic plants overexpressing *ATHB15* were indistinguishable from wild-type plants (data not shown). By contrast, antisense *ATHB15* transgenic plants were severely dwarfed with small, short rosette leaves (Figure 6a,b). Among 39 homozygous transgenic lines we obtained, 14 lines exhibited such phenotypic alterations, and four lines were lethally affected and died at the very early seedling stage. Others were mildly affected or similar to wild-type plants. Northern blot analysis showed that *ATHB15* is specifically suppressed but that other HD-ZIP III genes are unaffected in the antisense transgenic plants (Figure 6c). The phenotype of the antisense *ATHB15* transgenic plants may be again related to the arrested growth of homozygous

men1 lines. A slight downward curling of the leaf blade was also observed as in *men1/+*. This may have been caused by partial abaxialization of leaf polarity. Consistent with this view, the expression of *KANADI* and *YABBY* genes, which are abaxially expressed in leaf organs and in phloem tissues and regulate leaf polarity (Emery *et al.*, 2003; Eshed *et al.*, 2001; Kerstetter *et al.*, 2001; Sawa *et al.*, 1999; Siegfried *et al.*, 1999), was upregulated in *men1/+* and antisense *ATHB15* transgenic plants but repressed in *mATHB15* transgenic plants (data not shown). This altered expression may be caused by alterations in vascular organization as well as in leaf morphology.

It is apparent that *ATHB15* has a partially overlapping function with other HD-ZIP III genes such as *PHV* and *PHB* (McConnell and Barton, 1998; McConnell *et al.*, 2001) in the specification of leaf polarity, although its role is not as critical as that of *PHV* and *PHB*. Consistent with this notion, the adaxial and abaxial cell fate determination during vascular development is governed by a mechanism similar to that functioning in the formation of lateral organ polarity (Emery *et al.*, 2003; Juarez *et al.*, 2004).

Especially, many antisense *ATHB15* transgenic plants showed fasciated inflorescence stems (Figure 6a), further supporting the view that the fasciated inflorescence stems observed in *men1/+* are caused at least in part by miR166-mediated *ATHB15* repression. These observations suggest that *ATHB15* may have a role in apical meristem formation as well as in vascular development in inflorescence stems, which are developmentally related (Clark *et al.*, 1996; Laufs *et al.*, 1998; McHale and Koning, 2004).

Transverse sections of fully developed inflorescence stems at a growth stage of green siliques, which are routinely obtained 3 weeks after bolting (5.5-week-old plants) under our growth conditions, exhibit striking differences among *men1/+*, *mATHB15* transgenic plants, and wild-type plants. Lignified tissue was greatly expanded in *men1/+* and antisense *ATHB15* transgenic plants but was significantly reduced in *mATHB15* transgenic plants (Figure 6d). Lignified tissue formation is mainly contributed by the activity of fascicular cambium and interfascicular cambium that eventually differentiate into secondary xylem (Baima *et al.*, 2001), indicating that cambium activity and its differentiation into xylem is markedly promoted in *men1/+* and in antisense *ATHB15* transgenic plants.

The number of vascular bundles was also different. Whereas it was six to eight in wild-type plants, it was 11–12 in *men1/+* and antisense *ATHB15* transgenic plants and four to five in *mATHB15* transgenic plants (Figure 6d). This alteration may be due to the differences in stem size – fasciated stems may have more vascular bundles, and thinner stems may have fewer vascular bundles. However, the radial patterning of vascular bundles was unaltered, and the adaxial–abaxial polarity was maintained in both plants, although it was somewhat irregular. Amphivasal vascular bundles were observed in very few lines of *men1/+* and antisense *ATHB15* transgenic plants, unlike plants with the *REV* mutation (*avb1*) (Emery *et al.*, 2003; Zhong and Ye, 2004). These results indicate that *ATHB15* has distinct as well as overlapping functions compared with *REV*, *ATHB8*, and other HD-ZIP genes involved in vascular development.

It is also evident that *ATHB15* is necessary for vascular development, which is contrary to the role of *ATHB8*. The alteration of vascular bundles and vascular development observed in *men1/+* and *ATHB15* transgenic plants is also consistent with the localized expression of *ATHB15* in the procambial and cambial cells (Ohashi-Ito and Fukuda, 2003).

ATHB15 negatively regulates vascular cell differentiation

Close examination of individual vascular bundles revealed that the formation of xylem tissue and interfascicular tissue was greatly promoted in *men1/+* and antisense *ATHB15* transgenic

plants (Figure 7), consistent with the expanded lignification pattern (Figure 6d). Protoxylem and metaxylem were also greatly expanded. However, the phloem formation was only marginally affected by the *men1* mutation and by the antisense expression of *ATHB15*, although it was somewhat flattened compared with that in wild-type plants. Arabidopsis cambium produces more xylems than phloems (Baima *et al.*, 2001). The increased production of primary and secondary xylems is apparently caused by the acceleration of procambial/cambial cell differentiation into xylem parenchyma cells (Baima *et al.*, 2001).

Notably, vascular tissues, especially primary and secondary xylems, were very poorly developed in *mATHB15* transgenic plants (Figure 7). The number of vascular bundles was also fewer than in wild-type plants (Figure 6c), although the collateral organization of xylem and phloem was maintained in individual vascular bundles. These observations unequivocally demonstrate that *ATHB15* is important for vascular development and is responsible for its negative regulation. By contrast, *ATHB8*, which is exclusively expressed in xylem tissue, positively regulates vascular cell differentiation (Baima *et al.*, 2001). Consistent with this, the expansion of the lignified tissue in *men1/+* and antisense *ATHB15* transgenic plants is very similar to that of transgenic plants overexpressing *ATHB8* (Baima *et al.*, 2001). *ATHB15* and *ATHB8* may have antagonistic roles during vascular development.

Auxin induces *ATHB8* (Baima *et al.*, 1995) and stimulates vascular cell differentiation, suggesting that *ATHB8* mediates auxin signals in the promotion of vascular development (Sachs, 2000; Ye, 2002). However, auxin does not influence the expression of *ATHB15* and *MIR166a* (data not shown) under the same experimental conditions as used with *ATHB8* (Baima *et al.*, 1995). Our results indicate that *ATHB15* is essential for vascular development. Antisense overexpression of *ATHB15* causes severe dwarfism, as in the *men1* mutation, possibly due to the suppressed vascular system. Altogether, we propose a model for the regulation of vascular development in which miR166-mediated regulation of *ATHB15* is a primary molecular device for the proper maintenance of the vascular system, which is further modulated by *ATHB8* through both the posttranscriptional regulation by miR166 and the transcriptional regulation by auxin.

Discussion

miRNAs are emerging as critical post-transcriptional regulators in various plant developmental processes. Although the first plant miRNAs have been reported very recently (Llave *et al.*, 2002; Reinhart *et al.*, 2002), much later than those in animals, more miRNAs and their target genes have been identified and functionally characterized in plants.

One of the best characterized miRNAs in plants is miR166/165 and its target genes that encode the HD-ZIP III transcription factors (Baima *et al.*, 2001; Emery *et al.*, 2003; Kidner and Martienssen, 2004; McConnell and Barton, 1998; McConnell *et al.*, 2001). Dominant or semidominant gain-of-function mutations in *PHB*, *PHV*, and *REV* all map to the START domain that has a limited sequence similarity to sterol-binding proteins in metazoans. Furthermore, the presence of the miR166/165 complementary sequences within the START domain strongly supports the view that miRNA-directed post-transcriptional regulation of the target mRNAs is related to the phenotypic alterations of the mutants. This has been experimentally demonstrated by molecular genetic and biochemical studies of miRNA-resistant target genes. Although *ATHB15* has been suggested to have a role in vascular development (Ohashi-Ito and Fukuda, 2003), it has not been systematically examined yet.

In this work, we demonstrated that miR166 regulates *ATHB15* through mRNA cleavage during vascular development using a morphogenetic Arabidopsis mutant that is featured by fasciated inflorescence stems with altered vascular development. An *MIR166a* gene is activated by the

insertion of the CaMV 35S enhancer in the mutant. The transcript levels of *ATHB15*, *PHV*, *PHB*, and *ATHB8* were reduced in the mutant with the reduction of *ATHB15* mRNA most significant. Consistent with this, miR166 efficiently cleaves *ATHB15* mRNA *in planta* as well as *in vitro*.

Transgenic plants with reduced *ATHB15* expression are severely dwarfed with fasciated inflorescence stems as observed in *men1/+*. The vascular system is also altered by the *men1* mutation and by the reduction or overexpression of *ATHB15*. The expansion of lignified tissue was greatly promoted in *men1/+* and antisense *ATHB15* transgenic plants but significantly reduced in *mATHB15* transgenic plants (Figure 6d). The number of vascular bundles was also influenced. Altogether, it is evident that *ATHB15* is critical for vascular development and negatively regulates vascular cell differentiation.

However, the mechanisms that regulate vascular development are not simple. Several growth hormones have been demonstrated or implicated in vascular tissue formation and differentiation. A HD-ZIP III gene encoding an *ATHB8* homolog is mainly expressed in xylem cells and induced by brassinosteroids (BRs) in cultured *Z. elegans* cells (Ohashi-Ito *et al.*, 2002). Consistent with this, xylem development is reduced in BR-deficient Arabidopsis (Choe *et al.*, 1999). Brassinazole, a BR synthesis inhibitor, represses xylem formation (Nagata *et al.*, 2001). *ZeHB-13*, an *ATHB15* gene homolog in *Z. elegans*, is suppressed by brassinazole but reversed by the addition of BR, indicating that BR is not required for the *ZeHB-13* induction but promotes its expression (Ohashi-Ito and Fukuda, 2003). However, we could not observe any effects of brassinazole and BRs on *ATHB15* expression (data not shown). Auxin is the major signaling determinant in the development of vascular system in Arabidopsis. Its polar transport seems to promote the formation of vascular strands (Sachs, 1991). Some mutants with defective vascular system are caused by defects in auxin transport or auxin signaling (Berleth and Sachs, 2001; Dengler and Kang, 2001; Mahonen *et al.*, 2000). Notably, *ATHB8* that promotes cambial/procambial cell differentiation into xylem tissue is induced by auxin, indicating that *ATHB8* modulates auxin signals during vascular development (Baima *et al.*, 1995, 2001).

Both *ATHB15* and *ATHB8* are regulated by miR166 through mRNA cleavage (Figure 4b). However, *ATHB15* is distinct from *ATHB8* in several aspects. *ATHB15* does not respond to auxin, unlike *ATHB8*. Whereas *ATHB15* negatively regulates xylem tissue formation, *ATHB8* has a promoting effect on it. In addition, *ATHB15* is essential for vascular development, but *ATHB8* is not (Baima *et al.*, 2001). It is therefore hypothesized that miR166/165 is a modulator that balances *ATHB15* and *ATHB8* functions during vascular development. Auxin seems to further adjust the developmental process by transcriptionally regulating *ATHB8*. Analysis of double mutants of *ATHB15* and *ATHB8* or of transgenic plants overexpressing both *ATHB15* and *ATHB8*, in combination with auxin and auxin transport inhibitors, would clarify this hypothesis. Other HD-ZIP III genes seem to play additional roles in the fine regulation of vascular development. *PHV*, *PHB*, and *REV* regulate organ polarity by specifying adaxial (xylem) and abaxial (phloem) cell fates and ascertain vascular patterning (Emery *et al.*, 2003; Juarez *et al.*, 2004; Kidner and Martienssen, 2004; McConnell and Barton, 1998; McConnell *et al.*, 2001; Zhong and Ye, 2004).

Vascular system formation is a complex developmental process that is regulated by diverse genetic components and growth hormones. Furthermore, the pattern and organization of vascular systems are quite variable in different plant species. However, the molecular mechanisms that underlie the spatial and temporal regulation of vascular systems are probably shared by all vascular plants. The conserved basic architecture of vascular systems and HD-ZIP III genes in dicots, monocots, and moss (Floyd and Bowman, 2004) suggest that the

miR166-mediated regulation of vascular development via HD-ZIP III genes may be a general rule in all vascular plants.

Experimental procedures

Plant materials and growth conditions

All Arabidopsis plants used in this work were in the Columbia background (Col-0). Plants were grown in a controlled culture room at 24–25°C with a relative humidity of 60% in long-day condition (16 h light and 8 h dark). *Nicotiana benthamiana* was also grown in soil under the same growth conditions.

Transgenic Arabidopsis plants

Transgenic Arabidopsis plants were produced by a simplified floral dip method as described (Clough and Bent, 1995). Full-size cDNAs of sense and antisense *ATHB15* and *mATHB15* were expressed under the control of the CaMV 35S promoter in pBI121 (Clontech, Palo Alto, CA, USA). The P1/HC-Pro expression was also driven by the CaMV 35S promoter as described (Kasschau *et al.*, 2003). Homozygous transgenic lines were isolated through two additional generations after primary selection for each transformation.

Isolation of *men1* mutant

The *men1* mutant was isolated from an Arabidopsis mutant pool generated using the activation tagging vector pSKI015 as described (Weigel *et al.*, 2000). The T-DNA insertion site was mapped by the TAIL-PCR method (Liu *et al.*, 1995). The single insertion event of T-DNA in *men1* was confirmed by segregation analysis and by genomic Southern blot analysis using *SacI*-digested genomic DNAs and a genomic DNA fragment of 500 bp near the insertion site as a probe (Figure 3a).

miRNA Northern blot analysis

For miRNA Northern blot hybridization, total RNA was extracted from plant materials using the TRIzol reagent (Invitrogen, Carlsbad, CA, USA) according to the procedure previously described (Pfeffer *et al.*, 2003) but with some modifications. After isopropanol precipitation, the RNA pellet was briefly centrifuged without rinsing with ethanol, and the remaining isopropanol was completely removed by pipetting. The RNA pellet was then dissolved in 95% formamide/25 mM EDTA. We found that these steps greatly improve the yield and solubility of miRNA in total RNA preparations. Northern blot hybridizations were carried out using the ULTRA-Hyb Oligo solution according to the procedure supplied by the manufacturer (Ambion, Houston, TX, USA). The oligonucleotide probes were end-labeled at the 5'-end using P³²- γ -ATP and T4 polynucleotide kinase. An oligonucleotide complementary to 5S rRNA was also processed in the same way and used as a control.

Semiquantitative RT-PCR analyses of HD-ZIP III gene expression

The transcript levels of HD-ZIP III genes were analyzed by semiquantitative RT-PCR runs. Total RNA samples were extracted from aerial parts of plants and treated extensively with RNase-free DNase I to eliminate any contaminating genomic DNA. The first-strand cDNA was synthesized using Pfu Turbo polymerase (Stratagene, La Jolla, CA, USA) from 2 μ g of total RNA in a 20- μ l reaction volume, and 2 μ l of the reaction mixture was subject to subsequent PCR in a 50- μ l reaction volume. RT-PCR runs were 15–30 cycles, depending on the linear range of PCR amplification for each gene, each cycle at 94°C for 1 min, 60°C for 1 min, and 72°C for 4 min with a final cycle at 72°C for 10 min to allow the completion of polymerization. The PCR primer pairs were designed from the sequence regions of each gene with the least sequence identities among the HD-ZIP III genes. The primer sequences are 5'-

TCTTGCAAGGATGGTAAGTTGG (forward, F) and 5'-CTATTAGTCTGAGTAACCTCCTGAGC (reverse, R) for *ATHB15*, 5'-AGGAAGCAATAATAGTCACAATATGG (F) and 5'-ATACTGGCCCGTTTTGTGTATT (R) for *ATHB8*, 5'-CCATGGACGATAGAGACTCTCC (F) and 5'-ACCACTTCCAAAACCTTGGAAGA (R) for *PHV*, 5'-GAGATATGATGAACAGAGAGTCGCC (F) and 5'-ACCAAACCTTCCAGGGGACA (R) for *PHB*, and 5'-AACCACCGTGAGAGAAGCAGT (F) and 5'-CCGGAACATAGTGAAAACCTTC (R) for *REV*.

Analysis of *ATHB15* mRNA cleavage

Target mRNA cleavage by miR166 was examined in three different ways. For analysis in *N. benthamiana*, *Agrobacterium* cells containing plant expression vector constructs with either an *MIR166a* gene of about 170 bp or *ATHB15* target genes under the control of the CaMV 35S promoter were injected directly into leaves independently or in various combinations. Total RNAs were extracted from the leaf tissues at 4 days after injection as described (Llave *et al.*, 2000) and analyzed in a 1.2% formaldehyde-agarose gel. The Northern gel blots were probed with the putative 5'-end cleavage fragment labeled with digoxigenin-UTP by *in vitro* transcription with SP6 or T7 RNA polymerase using the DIG RNA Labeling Kit (Roche Applied Science, Penzberg, Germany).

For analysis in standard wheat germ extracts, a 5'-end labeled target RNA corresponding to a fragment of *ATHB15* mRNA spanning the miR166/165 cleavage site was incubated in wheat germ extracts under miRNA processing conditions as described (Tang *et al.*, 2003). Aliquots were removed at different time intervals, and products resolved in a 6% sequencing gel.

To map the *ATHB15* mRNA cleavage site *in vivo*, total RNAs were extracted from floral organs of *Arabidopsis*. The 5'-end of the cleavage product was determined by a modified RNA ligasemediated 5'-RACE method (Kasschau *et al.*, 2003; Llave *et al.*, 2002) using the RLM-RACE kit (Ambion).

Histochemical analysis

Transverse sectioning of 5.5-week-old inflorescence stems, 3 weeks after bolting under our growth conditions, and tissue staining were carried out essentially as described (Baima *et al.*, 2001) but using aniline blue for the analysis of vascular tissues and toluidine blue for the analysis of vascular bundles. The aniline blue-stained sections were observed under a fluorescence microscope, and the toluidine blue-stained sections were observed under a bright field microscope with appropriate magnification.

Acknowledgements

We thank Y.-H. Seo for plant culture and the members of the Molecular Signaling Laboratory for technical support and scientific discussion. This work was supported by the Brain Korea 21 program (KRF), the BioGreen21 program, grants from KOSEF (R02-2003-000-10001-0), KISTEP (M1-0219-00-0003), and the Plant Signaling Network Research Center, and NIH grant GM-44640 (to N.-H.C.). J.L.R. was supported by a Pew Latin American fellowship.

References

- Aukerman MJ, Sakai H. Regulation of flowering time and floral organ identity by a microRNA and its *APETALA2*-like target genes. *Plant Cell* 2003;15:2730–2741. [PubMed: 14555699]
- Baima S, Nobili F, Sessa G, Lucchetti S, Ruberti I, Morelli G. The expression of the *ATHB-8* homeobox gene is restricted to provascular cells in *Arabidopsis thaliana*. *Development* 1995;121:4171–4182. [PubMed: 8575317]

- Baima S, Possenti M, Matteucci A, Wisman E, Altamura MM, Ruberti I, Morelli G. The Arabidopsis ATHB-8 HD-Zip protein acts as a differentiation-promoting transcriptional factor of the vascular meristems. *Plant Physiol* 2001;126:643–655. [PubMed: 11402194]
- Bartel DP. MicroRNAs: genomics, biogenesis, mechanisms, and function. *Cell* 2004;116:281–297. [PubMed: 14744438]
- Bartel B, Bartel DP. MicroRNAs: at the root of plant development. *Plant Physiol* 2003;132:709–717. [PubMed: 12805599]
- Berleth T, Sachs T. Plant morphogenesis: long distance coordination and local patterning. *Curr Opin Plant Sci* 2001;4:57–62.
- Carland FM, Fujioka S, Takasato S, Yoshida S, Nelson T. The identification of *CVPI* reveals a role for sterols in vascular patterning. *Plant Cell* 2002;14:2045–2058. [PubMed: 12215504]
- Chen X. A microRNA as a translational repressor of *APETALA2* in Arabidopsis flower development. *Science* 2004;303:2022–2025. [PubMed: 12893888]
- Choe S, Dilkes BP, Gregory BD, et al. The Arabidopsis *dwarf1* mutant is defective in the conversion of 24-methylene-cholesterol to campesterol in brassinosteroid biosynthesis. *Plant Physiol* 1999;119:897–907. [PubMed: 10069828]
- Clark SE, Jacobsen SE, Levin JZ, Meyerowitz EM. The *CLAVATA* and *SHOOT MERISTEMLESS* loci competitively regulate meristem activity in Arabidopsis. *Development* 1996;122:1567–1575. [PubMed: 8625843]
- Clough SJ, Bent AF. Floral dip: a simplified method for *Agrobacterium*-mediated transformation of *Arabidopsis thaliana*. *Plant J* 1995;16:735–743. [PubMed: 10069079]
- Dengler N, Kang J. Vascular patterning and leaf shape. *Curr Opin Plant Sci* 2001;4:50–56.
- Emery JF, Floyd SK, Alvarez J, Eshed Y, Hawker NP, Izhaki A, Baum SF, Bowman JL. Radial patterning of Arabidopsis shoots by class III HD-ZIP and *KANADI* genes. *Curr Biol* 2003;13:1768–1774. [PubMed: 14561401]
- Esau, K.** (1965) *Plant Anatomy*, 2nd edn. New York, NY: John Wiley & Sons.
- Eshed Y, Baum SF, Perea JV, Bowman JL. Establishment of polarity in lateral organs of plants. *Curr Biol* 2001;11:1251–1260. [PubMed: 11525739]
- Floyd SK, Bowman JL. Ancient microRNA target sequences in plants. *Nature* 2004;428:485–486. [PubMed: 15057819]
- Jang JC, Fujioka S, Tasaka M, Seto H, Takasato S, Ishii A, Aida M, Yoshida S, Sheen J. A critical role of sterols in embryonic patterning and meristem programming revealed by the *fackel* mutants of *Arabidopsis thaliana*. *Genes Dev* 2000;14:1485–1497. [PubMed: 10859167]
- Juarez MT, Kul JS, Thomas J, Heller BA, Timmermans MCP. microRNA-mediated repression of *rolled leaf1* specifies maize leaf polarity. *Nature* 2004;428:84–88. [PubMed: 14999285]
- Kasschau KD, Xie Z, Allen E, Llave C, Chapman EJ, Krizan KA, Carrington JC. P1/HC-Pro, a viral suppressor of RNA silencing, interferes with Arabidopsis development and miRNA function. *Dev Cell* 2003;4:205–217. [PubMed: 12586064]
- Kerstetter RA, Bollman K, Tayler RA, Bomblies K, Poethig RS. *KANADI* regulates organ polarity in Arabidopsis. *Nature* 2001;411:706–709. [PubMed: 11395775]
- Kidner CA, Martienssen RA. Macro effects of micro RNAs in plants. *Trends Genet* 2003;19:13–16. [PubMed: 12493243]
- Kidner CA, Martienssen RA. Spatially restricted micro RNA directs leaf polarity through ARGONAUTE1. *Nature* 2004;428:81–84. [PubMed: 14999284]
- Laufs P, Dockx J, Kronenberger J, Traas J. *MGOUN1* and *MGOUN2*: two genes required for primordium initiation at the shoot apical and floral meristems in *Arabidopsis thaliana*. *Development* 1998;125:1253–1260. [PubMed: 9477323]
- Laufs P, Peaucelle A, Morin H, Traas J. MicroRNA regulation of the *CUC* genes is required for boundary size control in Arabidopsis meristems. *Development* 2004;131:4311–4322. [PubMed: 15294871]
- Liu YG, Mitsukawa N, Oosumi T, Whittier RF. Efficient isolation and mapping of *Arabidopsis thaliana* T-DNA insert junctions by thermal asymmetric interlaced PCR. *Plant J* 1995;8:457–463. [PubMed: 7550382]

- Llave C, Kasschau KD, Carrington JC. Virus-encoded suppressor of posttranscriptional gene silencing targets a maintenance step in the silencing pathway. *Proc Natl Acad Sci USA* 2000;97:13401–13406. [PubMed: 11078509]
- Llave C, Xie Z, Kasschau KD, Carrington JC. Cleavage of *Scarecrow-like* mRNA targets directed by a class of Arabidopsis miRNA. *Science* 2002;297:2053–2056. [PubMed: 12242443]
- Mahonen AR, Bonke M, Kauppinen L, Riikonen M, Benfey PN, Helariutta Y. A novel two-component hybrid molecule regulates vascular morphogenesis of the vascular root. *Genes Dev* 2000;14:2938–2943. [PubMed: 11114883]
- Mallory AC, Dugas DV, Bartel DP, Bartel B. Micro RNA regulation of NAC-domain targets is required for proper formation and separation of adjacent embryonic, vegetative, and floral organs. *Curr Biol* 2004a;14:1035–1046. [PubMed: 15202996]
- Mallory AC, Reinhart BJ, Jones-Rhoades MW, Tang G, Zamore PD, Barton MK, Bartel DP. MicroRNA control of *PHABULOSA* in leaf development: importance of pairing to the microRNA 5' region. *EMBO J* 2004b;23:3356–3364. [PubMed: 15282547]
- McConnell JR, Barton MK. Leaf polarity and meristem formation in Arabidopsis. *Development* 1998;125:2935–2942. [PubMed: 9655815]
- McConnell JR, Emery JF, Eshed Y, Bao N, Bowman J, Barton MK. Role of *PHABULOSA* and *PHAVOLUTA* in determining radial patterning in shoots. *Nature* 2001;411:709–712. [PubMed: 11395776]
- McHale N, Koning E. MicroRNA-directed cleavage of *Nicotiana sylvestris* *PHAVOLUTA* mRNA regulates the vascular cambium and structure of apical meristems. *Plant Cell* 2004;16:1730–1740. [PubMed: 15194817]
- Nagata N, Asami T, Yoshida S. Brassinazole, an inhibitor of brassinosteroid biosynthesis, inhibits development of secondary xylem in cross plants. *Plant Cell Physiol* 2001;42:1006–1011. [PubMed: 11577196]
- Ohashi-Ito K, Fukuda H. HD-zip III homeobox genes that include a novel member, *ZeHB-13* (*Zinnia*)/*ATHB-15* (Arabidopsis), are involved in procambium and xylem cell differentiation. *Plant Cell Physiol* 2003;44:1350–1358. [PubMed: 14701930]
- Ohashi-Ito K, Demura T, Fukuda H. Promotion of transcript accumulation of novel *Zinnia* immature xylem-specific HD-Zip III homeobox genes by brassinosteroids. *Plant Cell Physiol* 2002;43:1146–1153. [PubMed: 12407194]
- Otsuga D, DeGuzman B, Prigge MJ, Drews GN, Clark SE. *REVOLUTA* regulates meristem initiation at lateral positions. *Plant J* 2001;25:223–236. [PubMed: 11169198]
- Palatnik JF, Allen E, Wu X, Schommer C, Schwab R, Carrington JC, Weigel D. Control of leaf morphogenesis by microRNAs. *Nature* 2003;425:257–263. [PubMed: 12931144]
- Pfeffer, S., Lagos-Quintana, M. and Tuschl, T.** (2003) Cloning of small RNA molecules. In *Current Protocols in Molecular Biology* (Ausubel, F.M., Brent, R., Kingston, R.E., Moore, D.D., Seidmann, J.G., Smith, J.A. and Struhl, K. eds). New York, NY: John Wiley & Sons. pp. 26.4.1–26.4.18.
- Ponting CP, Aravind L. START: a lipid-binding domain in StAR, HD-ZIP and signaling proteins. *Trends Biochem Sci* 1999;24:130–132. [PubMed: 10322415]
- Reinhart BJ, Weinstein EG, Rhoades MW, Bartel B, Bartel DP. MicroRNAs in plants. *Genes Dev* 2002;16:1616–1626. [PubMed: 12101121]
- Rhoades MW, Reinhart BJ, Lim LP, Burge CB, Bartel B, Bartel DP. Prediction of plant microRNA targets. *Cell* 2002;110:513–520. [PubMed: 12202040]
- Sachs T. Cell polarity and tissue patterning in plants. *Dev Suppl* 1991;1:83–93.
- Sachs T. Integrating cellular and organismic aspects of vascular differentiation. *Plant Cell Physiol* 2000;41:649–656. [PubMed: 10945333]
- Sawa S, Watanabe K, Goto K, Liu YG, Shibata D, Kanaya E, Morita EH, Okada K. *FILAMENTOUS FLOWER*, a meristem and organ identity gene of Arabidopsis, encodes a protein with a zinc finger and HMG-related domains. *Genes Dev* 1999;13:1079–1088. [PubMed: 10323860]
- Siegfried KR, Eshed Y, Baum SF, Ostuga D, Drews GN, Bowman JL. Members of the *YABBY* gene family specify abaxial cell fate in Arabidopsis. *Development* 1999;126:4117–4128. [PubMed: 10457020]

- Steeves, T.A. and Sussex, I.M.** (1989) *Patterns in Plant Development*, 2nd edn. Cambridge, UK: Cambridge University Press.
- Tang G, Reinhart B, Bartel DP, Zamore PD. A biochemical framework for RNA silencing in plants. *Genes Dev* 2003;17:49–63. [PubMed: 12514099]
- Vaucheret H, Vazquez F, Cr  t   P, Bartel DP. The action of *ARGONAUTE1* in the miRNA pathway and its regulation by the miRNA pathway are crucial for plant development. *Genes Dev* 2004;18:1187–1197. [PubMed: 15131082]
- Weigel D, Ahn JH, Bl  zquez MA, et al. Activation tagging in Arabidopsis. *Plant Physiol* 2000;122:1003–1013. [PubMed: 10759496]
- Ye ZH. Vascular tissue differentiation and pattern formation in plants. *Annu Rev Plant Biol* 2002;53:183–202. [PubMed: 12221972]
- Zhong R, Ye ZH. *amphival vascular bundle 1*, a gain-of-function mutation of the *IFL1/REV* gene, is associated with alterations in the polarity of leaves, stems, and carpels. *Plant Cell Physiol* 2004;45:369–385. [PubMed: 15111711]



Figure 1. *men1/+* plants with fasciated stem, enlarged meristem, and short carpel
Adult plants are shown. Inset shows a magnified image of the upper part of a fasciated inflorescence stem.

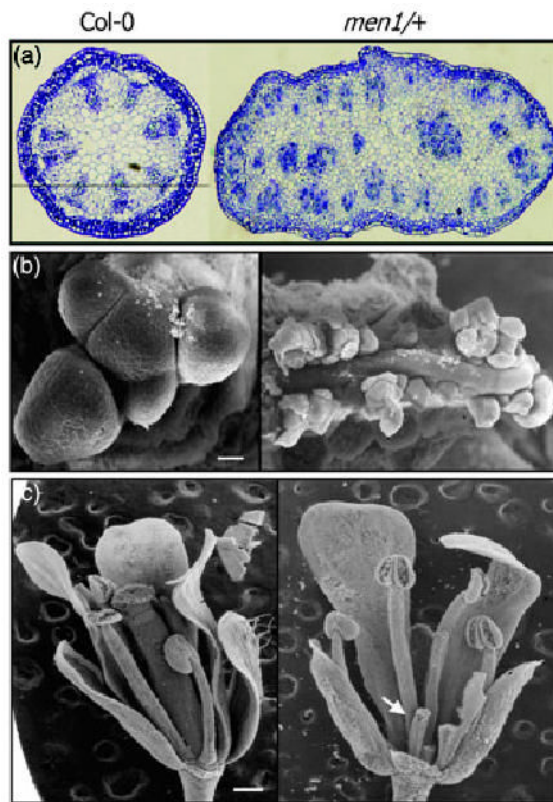


Figure 2. Inflorescence stem morphology and floral structure

(a) Transverse inflorescence stem sections stained with toluidine blue. Note that vascular patterning is disrupted in *men1/+*.

(b) Scanning electron microscopic (SEM) images of shoot apical meristems. Scale bar is 20 μm .

(c) SEM images of flowers. Some sepals and petals were removed to expose carpels. Carpel is extremely short in *men1/+* (arrow). Scale bar is 200 μm .

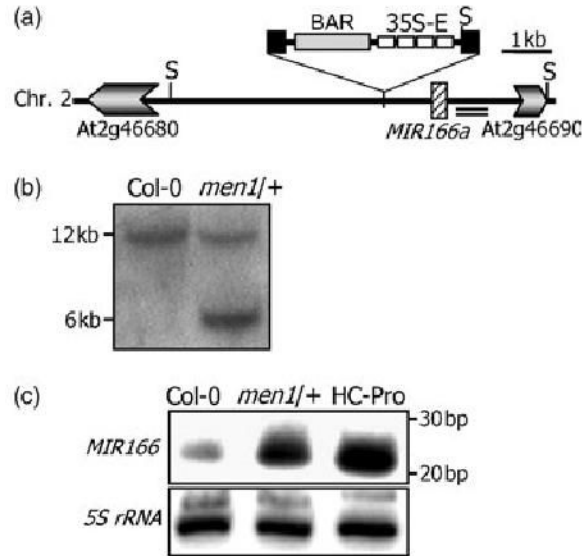


Figure 3. Activation tagging of an *MIR166a* gene in *men1/+*

(a) The 35S enhancer insertion site relative to the *MIR166a* locus. The double underlining indicates a 500-bp genomic DNA fragment used as a probe for genomic Southern blot analysis. S, *SacI* site.

(b) Genomic Southern blot analysis. *SacI*-digested genomic DNA was probed with a genomic DNA fragment.

(c) miR166 expression in *men1/+* and wild-type plants. Plants overexpressing tobacco etch virus (TEV) helper component proteinase (HC-Pro) were included as a comparison. Fifteen micrograms of total RNA was loaded onto each lane. 5S rRNA gene was used as a loading control.

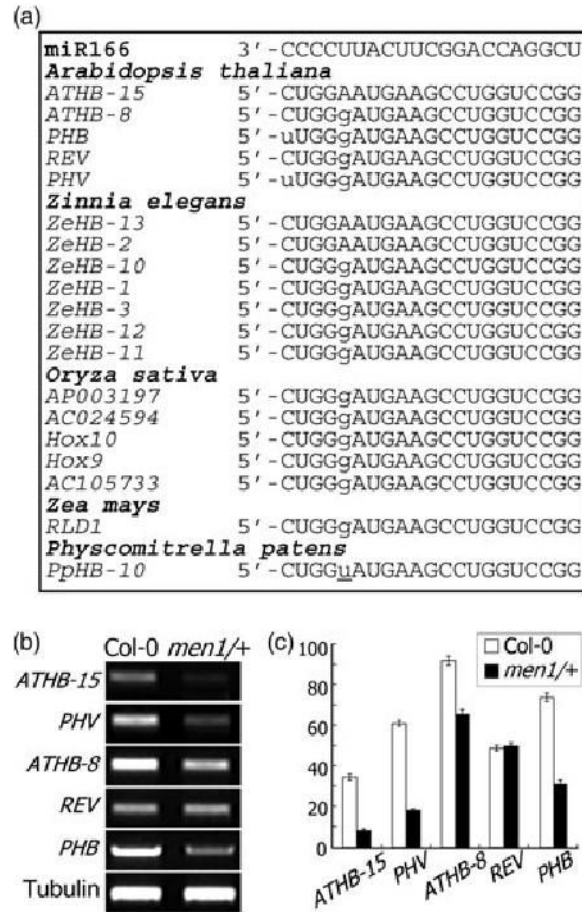


Figure 4. Transcript levels of HD-ZIP III genes in *men1/+*

(a) Sequence comparison of miR166 and its putative target sequences. The sequences of *ATHB15* gene homologs from plants and moss were aligned.

(b) Transcript levels of HD-ZIP III genes in *men1/+*.

(c) Graphic view of the transcript levels as measured in (b).

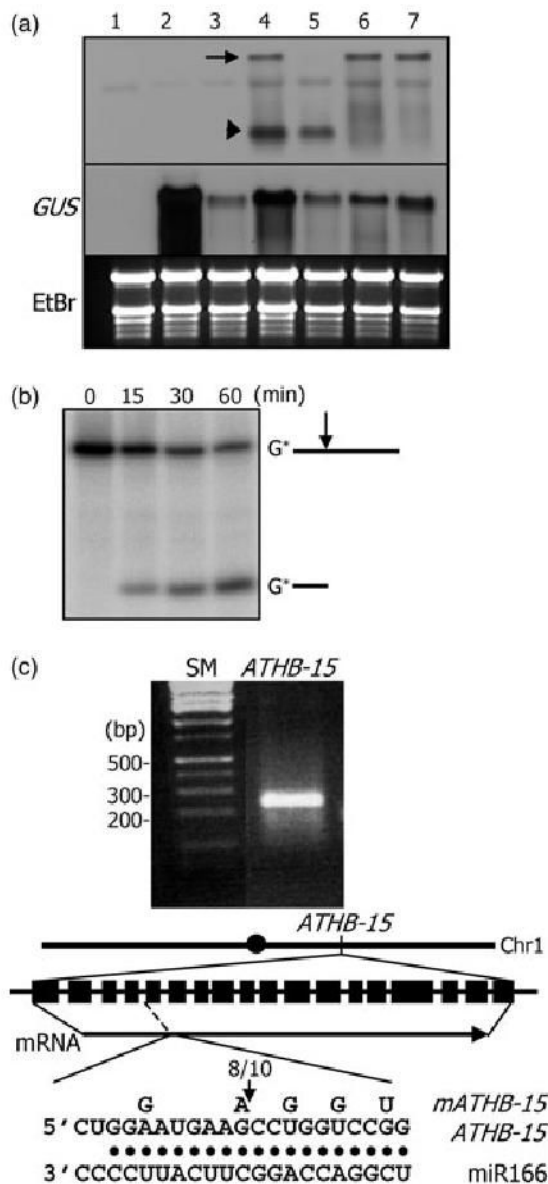


Figure 5. *ATHB15* mRNA cleavage by miR166 in *Nicotiana benthamiana*, wheat germ extract, and in Arabidopsis

(a) *ATHB15* mRNA cleavage in *N. benthamiana*. Total RNAs were extracted from plants without any vector constructs (1), with pBI121 control alone (2), with pBI121 + miR166 vector (3), with pBI121 + *ATHB15* vector (4), with pBI121 + *ATHB15* vector + miR166 vector (5), with pBI121 + *mATHB15* vector (6), and with pBI121 + *mATHB15* vector + miR166 vector (7). RNA gel blots were probed with the 5'-end cleavage fragment of *ATHB15*. The arrow marks the full-size mRNA, and the arrowhead the 5'-end cleavage product.

(b) *ATHB15* mRNA cleavage in wheat germ extract. A 5'-end labeled *ATHB15*- specific RNA was used in the assay.

(c) 5'-RACE to determine the cleavage site in Arabidopsis. The arrow in the diagram marks the cleavage site. The number refers to that of independent clones with the 5'-end as determined.

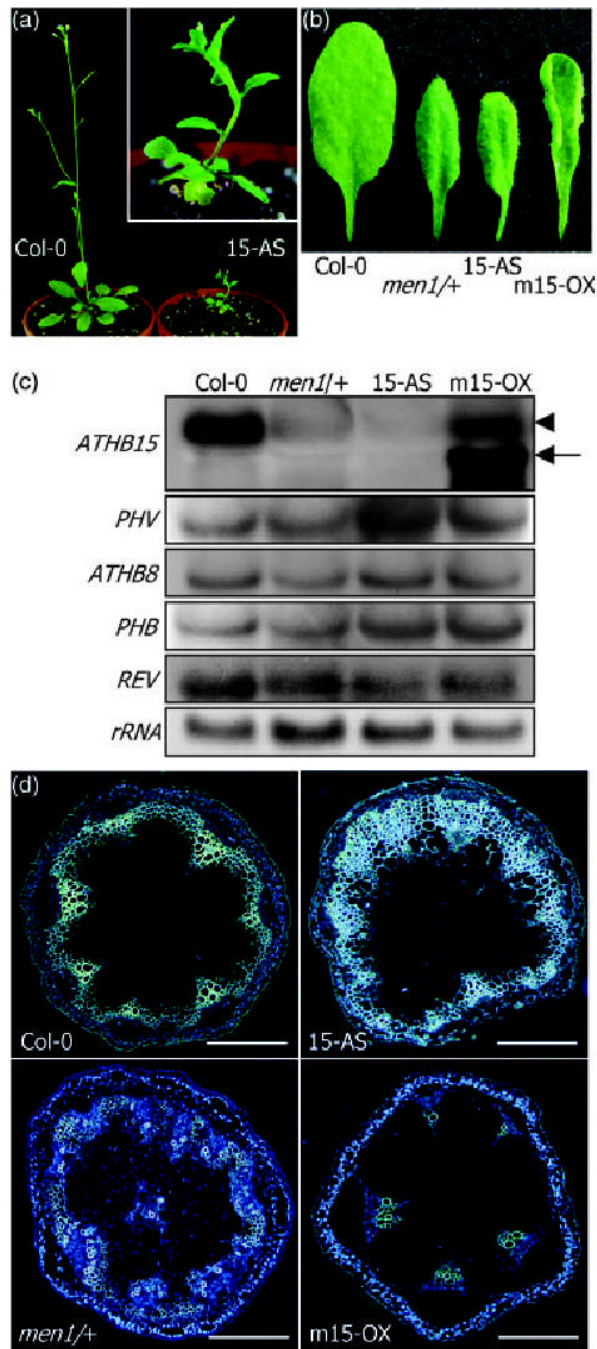


Figure 6. *ATHB15* transgenic plants and transverse sections of inflorescence stems

(a) Antisense *ATHB15* transgenic plant. Note the fasciated inflorescence stem in antisense *ATHB15* transgenic plant, although not as prominent as that in *men1/+*.

(b) Leaf morphology. Upward leaf curling is observed in *mATHB15* overexpressors, whereas a slight downward curling is evident in *men1/+* and antisense *ATHB15* transgenic plants.

(c) Transgene expressions. Expression of *ATHB15* transgenes was confirmed by Northern blot hybridization. Note that the sizes of transgene transcripts (arrow) are smaller than that of intrinsic *ATHB15* transcript (arrowhead). Expression of endogenous HD-ZIP III genes was also analyzed by Northern blot hybridizations.

(d) Transverse sections of inflorescence stems of 5.5-week-old plants. Sections were stained with aniline blue and observed under a fluorescence microscope. Scale bar is 20 μm .

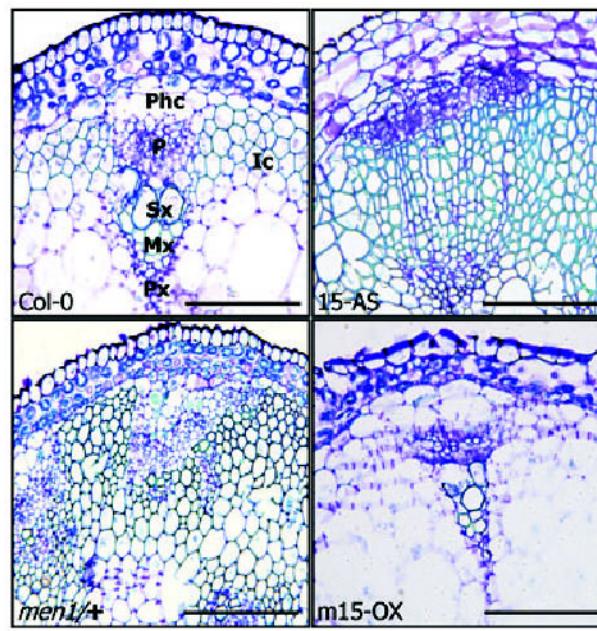


Figure 7. Vascular bundles in *men1/+* and *ATHB15* transgenic plants. Transverse sections were stained with toluidine blue and observed under a bright-field microscope. Phc, phloem cap cell; P, phloem; Sx, secondary xylem; Mx, metaxylem; Px, Protoxylem; Ic, interfascicular cells. Scale bars are 5 μ m.